



OPEN

# Anti-inflammatory effect of gold nanoparticles supported on metal oxides

Takashi Fujita<sup>1,2</sup>, Maeva Zysman<sup>3,4,5</sup>, Dan Elgrabli<sup>3,6</sup>, Toru Murayama<sup>1</sup>, Masatake Haruta<sup>1</sup>, Sophie Lanone<sup>3</sup>, Tamao Ishida<sup>1</sup> & Jorge Boczkowski<sup>3,7</sup>

Gold (Au) can be deposited as nanoparticles (NPs) smaller than 10 nm in diameter on a variety of metal oxide (MOx) NPs. Au/MOx have high catalytic performance and selective oxidation capacity which could have implications in terms of biological activity, and more specifically in modulation of the inflammatory reaction. Therefore, the aim of this study was to examine the effect of Au/TiO<sub>2</sub>, Au/ZrO<sub>2</sub> and Au/CeO<sub>2</sub> on viability, phagocytic capacity and inflammatory profile (TNF- $\alpha$  and IL-1 $\beta$  secretion) of murine macrophages. The most important result of this study is an anti-inflammatory effect of Au/MOx depending on the MOx nature with particle internalization and no alteration of cell viability and phagocytosis. The effect was dependent on the MOx NPs chemical nature (Au/TiO<sub>2</sub> > Au/ZrO<sub>2</sub> > Au/CeO<sub>2</sub> if we consider the number of cytokines whose concentration was reduced by the NPs), and on the inflammatory mediator considered. The effect of Au/TiO<sub>2</sub> NPs was not related to Au NPs size (at least in the case of Au/TiO<sub>2</sub> NPs in the range of 3–8 nm). To the best of our knowledge, this is the first demonstration of an anti-inflammatory effect of Au/MOx.

Gold (Au) can be deposited as nanoparticles (NPs) smaller than 10 nm in diameter on a variety of metal oxide (MOx) NPs (Au/MOx) (see Fig. S1 as an example). Au/MOx have attracted much attention due to their high catalytic performance for such as room temperature CO oxidation and selective oxidations in liquid phase<sup>1,2</sup>. The catalytic activity of Au strongly depends on the kind of support. For example, although TiO<sub>2</sub> is almost inactive for CO oxidation, the deposition of Au NPs onto TiO<sub>2</sub> enables to catalyze CO oxidation at room temperature<sup>3,4</sup>. The selective oxidation of glucose by Au supported on activated carbon or metal oxides has been a very active research area, as the transformation of readily available glucose to valuable gluconic acid is of great importance<sup>5,6</sup>.

These data in the field of heterogeneous catalysis have firmly established that deposition of Au on MOx NPs increases dramatically the intrinsic catalytic activity and this could also be the case for the biological activity. For example, Menchon et al.<sup>7</sup> reported that Au/CeO<sub>2</sub> exhibits antioxidant activity against reactive oxygen species (ROS) in Hep3B and HeLa cell related lines due to a peroxidase activity. Since the inflammatory reaction is highly dependent on oxidative stress<sup>8</sup> one can hypothesize that, in addition to their antioxidant properties, Au/MOx can have anti-inflammatory effects. Such an effect could have important implications in terms of medical utilization of Au/MOx. However, to the best of our knowledge no data on this effect is available in the current literature.

Therefore, in the present study we examined the effect of Au/MOx on cytotoxic and inflammatory response of macrophages, a key cell type involved in the inflammatory reaction. We used murine macrophages and investigated the roles of the size of Au NPs, the chemical nature of the supporting MOx NPs, and the kinetics of Au/MOx interference with the inflammatory reaction.

## Results

**Physicochemical properties of Au/MOx.** Physicochemical properties of Au/MOx are summarized in Table 1. Sizes of primary particles of MOx (TiO<sub>2</sub>, ZrO<sub>2</sub>, and CeO<sub>2</sub>) were in the range of 7–26 nm but MOx NPs are generally agglomerated to form secondary micrometer-sized (2.4–9.4  $\mu$ m) particles. Actual gold loading amounts of Au/MOx were ca. 1 wt% for all samples. The average sizes of Au NPs on TiO<sub>2</sub> and ZrO<sub>2</sub> prepared by

<sup>1</sup>Department of Applied Chemistry for Environment, Graduate School of Urban Environmental Sciences, Tokyo Metropolitan University, 1-1 Minami-osawa, Hachioji, Tokyo 192-0397, Japan. <sup>2</sup>Department of Applied Chemistry, School of Engineering, Tokyo University of Technology, 1401-1 Katakura, Hachioji, Tokyo 192-0982, Japan. <sup>3</sup>Univ Paris est Creteil, INSERM, IMRB, 94010 Creteil, France. <sup>4</sup>Univ Bordeaux, Centre de Recherche Cardio-Thoracique de Bordeaux, U1045, CIC, 1401 Bordeaux, France. <sup>5</sup>Service des Maladies Respiratoires, CHU Bordeaux, Bordeaux, France. <sup>6</sup>SAS NaorInnov, Courbevoie, France. <sup>7</sup>AP-HP, Hopital Henri Mondor, Antenne de Pneumologie, 94010 Creteil, France. ✉email: fujitats@stf.teu.ac.jp; jorge.boczkowski@inserm.fr

	Specific surface area /m <sup>2</sup> /g <sup>a</sup>	Primary particle size of metal oxide/nm <sup>b</sup>	Secondary particle size of metal oxide/μm <sup>c</sup>	Au loading/wt% <sup>d</sup>	Au particle size/nm <sup>e</sup>
Au3/TiO <sub>2</sub>	54	26	9.4	0.96	3.3 ± 1.4
Au8/TiO <sub>2</sub>	54	26	9.4	1.18	7.8 ± 2.7
Au/ZrO <sub>2</sub>	94	11	3.6	0.97	3.3 ± 1.8
Au/CeO <sub>2</sub>	114	7.3	2.4	0.96	No data <sup>f</sup>

**Table 1.** Physicochemical properties of Au NPs supported on metal oxides. <sup>a</sup>Specific surface area of metal oxide was calculated from N<sub>2</sub> adsorption isotherms using the Brunauer–Emmett–Teller (BET) method. <sup>b</sup>Primary particle size of metal oxide was estimated from the specific surface area. <sup>c</sup>Secondary particle size of metal oxide after the deposition of Au NPs was measured by dynamic laser scattering. <sup>d</sup>Actual loading amount of Au was determined by inductively coupled plasma-atomic emission spectroscopy (ICP-AES) or atomic absorption spectrometry (AAS). <sup>e</sup>Average particle size of Au NPs on metal oxides were estimated by HAADF-STEM. <sup>f</sup>Majority of Au species was considered to be atomically dispersed on CeO<sub>2</sub> and could not be detected due to a limitation of resolution and low contrast between heavy Ce and Au atoms by TEM.

deposition–precipitation were both of 3.3 nm. To examine the size effect of Au NPs, Au NPs with an average size of 8 nm were deposited on TiO<sub>2</sub> by solid grinding. High-angle annular dark-field scanning transmission electron microscopic (HAADF-STEM) images of Au/MOx are shown in Fig. 1. For Au/TiO<sub>2</sub> and Au/ZrO<sub>2</sub>, Au NPs were highly dispersed on MOx NPs. On CeO<sub>2</sub>, the most of Au species is atomically dispersed but only small amount Au NPs with ca. 20 nm in diameter was observed (Fig. 1d).

**No cytotoxic effect of Au/TiO<sub>2</sub> NPs on mouse macrophages.** Since Au/TiO<sub>2</sub> has been extensively studied in the field of catalysis<sup>1,3,4</sup> we have first compared biological effects of Au/TiO<sub>2</sub> samples having different size of Au NPs versus TiO<sub>2</sub> NPs on mouse peritoneal macrophages. Au NPs with two different mean diameters (3 and 8 nm) supported on pristine TiO<sub>2</sub> NPs were termed Au3/TiO<sub>2</sub> and Au8/TiO<sub>2</sub>, respectively. No cytotoxicity was observed by either 3-[4,5-dimethylthiazol-2-yl]-2,5 diphenyl tetrazolium bromide (MTT) or lactate dehydrogenase (LDH) release assays for TiO<sub>2</sub> and Au/TiO<sub>2</sub> NPs regardless of the concentration (1 to 100 μg ml<sup>-1</sup>), the exposure time (24 and 48 h) and the size of Au NPs (Fig. 2).

In addition to cytotoxicity evaluation, we examined whether Au/TiO<sub>2</sub> NPs modified the phagocytic capacity of macrophages (an important function of these cells) as compared to TiO<sub>2</sub> NPs. This was performed by quantifying phagocytosis of fluorescent beads after cells incubation with TiO<sub>2</sub> and Au/TiO<sub>2</sub> NPs (50 μg ml<sup>-1</sup>, 6 h incubation). The results of these experiments showed both TiO<sub>2</sub> and Au/TiO<sub>2</sub> NPs significantly increased the phagocytosis of fluorescent beads by peritoneal macrophages, but the differences between TiO<sub>2</sub> and Au/TiO<sub>2</sub> was not observed. This result shows that Au NPs did not modulate phagocytic capacity of macrophages (an important function of these cells).

Macrophages incubation with TiO<sub>2</sub> and Au/TiO<sub>2</sub> NPs significantly and similarly increased the phagocytosis of fluorescent beads by peritoneal macrophages (Fig. S2).

**TiO<sub>2</sub> and Au/TiO<sub>2</sub> NPs are internalized in mouse peritoneal macrophages.** Cellular uptake and intracellular morphology upon 24 h exposure to TiO<sub>2</sub> and Au/TiO<sub>2</sub> NPs were investigated in ultra-thin sections of resin-embedded cells using TEM.

TiO<sub>2</sub> NPs and Au/TiO<sub>2</sub> NPs (50 μg ml<sup>-1</sup>) were internalized in cells. The prevalent localization of NPs agglomerates was observed in cell vacuoles (Fig. S3). In accordance with the previous paragraph showing a lack of cytotoxicity, no morphologic sign of cell damage was observed.

**No inflammation induced by Au/TiO<sub>2</sub> NPs.** Incubation of mouse peritoneal macrophages with TiO<sub>2</sub> NPs (50 μg ml<sup>-1</sup>, 6 h), induced a significant increase in the concentration of TNF-α and IL-1β, two main pro-inflammatory cytokines, in cell culture medium (Fig. 4). In contrast, the deposition of Au NPs onto TiO<sub>2</sub> greatly reduced the concentration of both TNF-α and IL-1β as compared to pristine TiO<sub>2</sub>, and this effect was independent on the size of Au NPs.

**Au/TiO<sub>2</sub> NPs attenuate lipopolysaccharide (LPS)-induced inflammation.** Having demonstrated that Au/TiO<sub>2</sub> NPs did not elicit an inflammatory reaction, we questioned whether Au/TiO<sub>2</sub> NPs could blunt inflammation induced in a model of pathophysiological relevance, such as macrophages exposure to *Escherichia Coli* LPS. Since no difference of anti-inflammatory effect was observed between Au3/TiO<sub>2</sub> and Au8/TiO<sub>2</sub>, we investigated the effects of Au3/TiO<sub>2</sub> NPs (referred to as Au/TiO<sub>2</sub> in the following experiments). Mouse peritoneal macrophages were incubated with culture media for 6 h (control condition) or LPS for 2 h, and then the following 4 h with LPS alone or LPS plus TiO<sub>2</sub> or Au/TiO<sub>2</sub>. Taking into account the results presented in the previous paragraph, TNF-α and IL-1β cell culture supernatant concentrations were measured as a surrogate of the inflammatory reaction. As expected, incubation of cells with LPS for 2 + 4 h induced a significant increase as compared to the control condition (p < 0.05, Fig. 5a,b). Incubation of LPS followed by TiO<sub>2</sub> NPs did not significantly modify the effect of LPS alone. By contrast, this last effect was significantly attenuated by macrophage incubation with Au/TiO<sub>2</sub> NPs (p < 0.05, Fig. 5a,b). These results show that Au/TiO<sub>2</sub> can attenuate LPS induced inflammation, even when cells are incubated with these NPs after incubation with LPS.

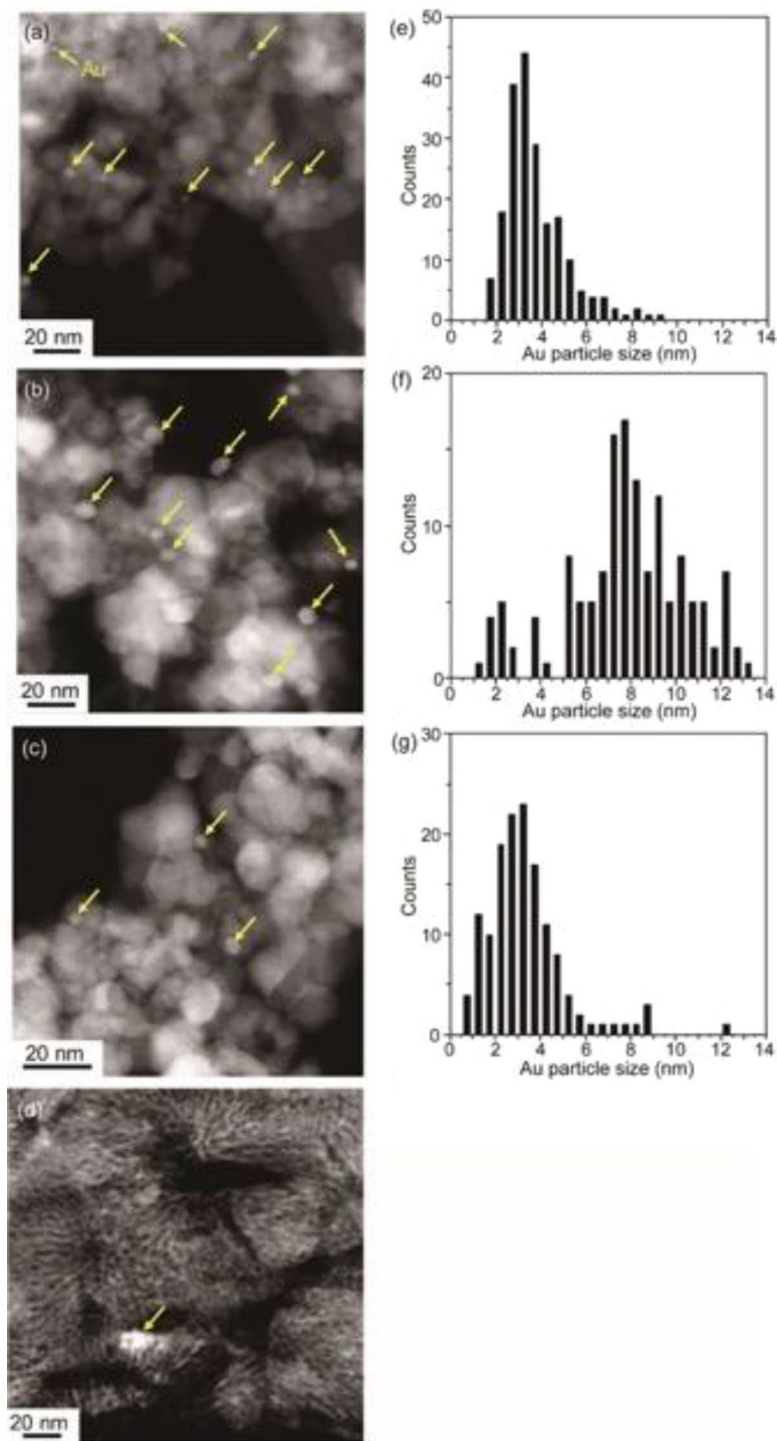


**Figure 1.** HAADF-STEM images of Au<sub>3</sub>/TiO<sub>2</sub> (a), Au<sub>8</sub>/TiO<sub>2</sub> (b), Au/ZrO<sub>2</sub> (c), Au/CeO<sub>2</sub> (d) and their size distributions of Au nanoparticles for Au<sub>3</sub>/TiO<sub>2</sub> (e), Au<sub>8</sub>/TiO<sub>2</sub> (f), and Au/ZrO<sub>2</sub> (g). Au nanoparticles were observed as brighter spots and yellow arrows indicate the Au nanoparticles. Only small amount of large Au aggregates was found in Au/CeO<sub>2</sub>.

**Effects of Au/ZrO<sub>2</sub> and Au/CeO<sub>2</sub> NPs on LPS-induced inflammation.** After showing the anti-inflammatory effect of Au/TiO<sub>2</sub> NPs, we investigated if this effect was related to the chemical nature of the MOx NPs. To answer this question, we examined the effect of Au NPs deposited on either ZrO<sub>2</sub> or CeO<sub>2</sub> NPs on mouse peritoneal macrophages. Physicochemical characterization of these Au/MOx are provided in Table 1. No effect of these NPs on macrophages viability was observed (Fig. 3).

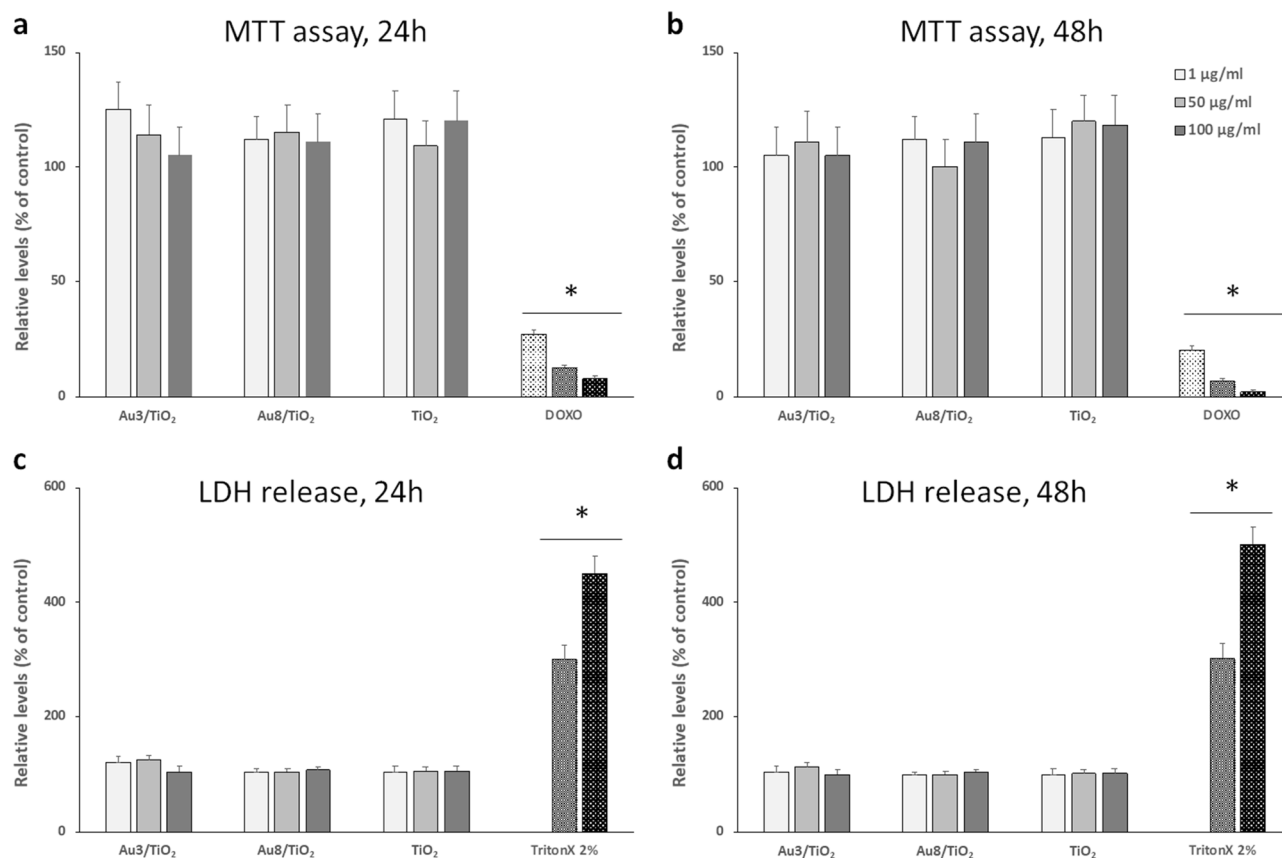


**Figure 2.** Cytotoxicity of Au nanoparticles (NPs) with two different diameters (3 and 8 nm respectively) supported on pristine  $\text{TiO}_2$  ( $\text{Au}_3/\text{TiO}_2$  and  $\text{Au}_8/\text{TiO}_2$  respectively) and  $\text{TiO}_2$  NPs alone on mouse peritoneal macrophages. Cell viability was measured using the MTT assay (**a,b**) and LDH relargage (**c,d**) after 24 and 48 h incubation (panels a and c, and b and d, respectively). Data are expressed as percentage of control condition (without NPs, 100% is the reference value) and are represented as mean  $\pm$  standard error of the mean (SEM) of 6 independent experiments. Positive controls are doxorubicine (DOXO, 1, 5 and 10  $\mu\text{g ml}^{-1}$ ) and TritonX-100 (10 vol. %). \* significantly different from control ( $p < 0.05$ ).

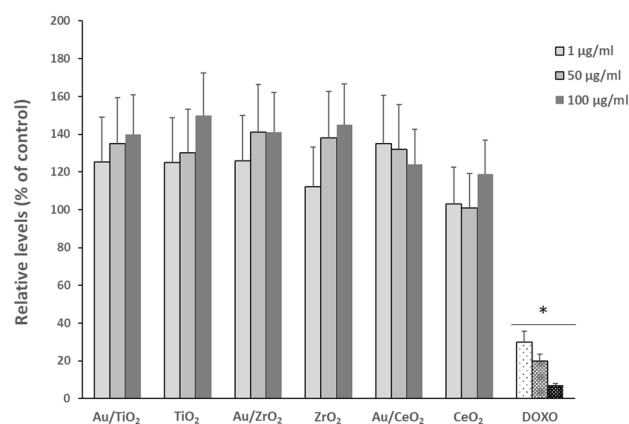


**Figure 3.** Cytotoxicity of Au nanoparticles (NPs) supported on  $\text{TiO}_2$ ,  $\text{ZrO}_2$  and  $\text{CeO}_2$  NPs and  $\text{TiO}_2$ ,  $\text{ZrO}_2$  and  $\text{CeO}_2$  NPs alone on mouse peritoneal macrophages. Cell viability was measured using the WST-1 assay after 24 h incubation. Data are expressed as percentage of control condition (without NPs, 100% is the reference value) and are represented as mean  $\pm$  SEM of 6 independent experiments. Positive control is doxorubicine (DOXO, 1, 5 and 10  $\mu\text{g ml}^{-1}$ ) \* significantly different from control ( $p < 0.05$ ).

Nanoparticle	Mean values $\pm$ SEM	Statistical significance
Au/TiO <sub>2</sub>	12,068 $\pm$ 499	*
TiO <sub>2</sub>	13,547 $\pm$ 340	
Au/ZrO <sub>2</sub>	9170 $\pm$ 109	**
ZrO <sub>2</sub>	13,538 $\pm$ 129	
Au/CeO <sub>2</sub>	12,743 $\pm$ 340	
CeO <sub>2</sub>	12,583 $\pm$ 255	#

**Table 2.** Reactive oxygen species (ROS) production in RAW 264.7 cells after expositions to different NPs. The final concentration of NPs was 50  $\mu\text{g ml}^{-1}$ . Amounts of ROS production were evaluated by the DCFH-DA ( $n = 7$ ). \* $p < 0.05$  vs TiO<sub>2</sub>, \*\* $p < 0.01$  vs ZrO<sub>2</sub>, # $p < 0.05$  vs TiO<sub>2</sub> and ZrO<sub>2</sub>.

Concerning LPS-induced inflammation, no effect was observed with Au/CeO<sub>2</sub> NPs, whereas Au/ZrO<sub>2</sub> NPs attenuated LPS-induced IL-1 $\beta$  production without any effect on TNF- $\alpha$  concentration (Fig. 5a,b). Therefore, we can conclude that Au/MOx possess an anti-inflammatory effect which depends on the nature of the MOx NPs and on the inflammatory mediator examined.

**Is the anti-inflammatory effect of Au/MOx NP related to cytokines adsorption on their surface?** We investigated the mechanisms underlying the anti-inflammatory effect of Au/MOx. Since MOx NPs adsorb different proteins on their surfaces<sup>9</sup>, we then investigated if the decreased concentration of LPS-induced TNF- $\alpha$  and IL-1 $\beta$  concentration observed with Au/TiO<sub>2</sub> and Au/ZrO<sub>2</sub> (only for IL-1 $\beta$  in this last case) was related to adsorption of these cytokines on these Au/MOx. The results of these experiments showed that incubation of each cytokine with the different Au/MOx did not change its respective concentration when compared to the MOx NPs without Au (Fig. 6). This result excludes cytokines adsorption as a mechanism explaining the anti-inflammatory effect of Au/TiO<sub>2</sub> and Au/ZrO<sub>2</sub>.

**Is the anti-inflammatory effect of Au/MOx related to their antioxidant properties?** We then examined if the anti-inflammatory effect of Au/TiO<sub>2</sub> and Au/ZrO<sub>2</sub> was related to antioxidant properties, as demonstrated in other conditions<sup>10,11</sup>. To investigate this issue, we measured the effect of Au/MOx NPs on intracellular reactive oxygen species (ROS) concentration. These experiments showed that intracellular ROS production induced by Au/TiO<sub>2</sub> and Au/ZrO<sub>2</sub> NPs was smaller than that of TiO<sub>2</sub> and ZrO<sub>2</sub> respectively, demonstrating an antioxidant effect of Au/TiO<sub>2</sub> and Au/ZrO<sub>2</sub> (Table 2), in accordance with their (partial) anti-inflammatory effect. This effect was more pronounced in the case of Au/ZrO<sub>2</sub> compared to Au/TiO<sub>2</sub> (mean reduction of 32% vs 11% compared to ZrO<sub>2</sub> and TiO<sub>2</sub> respectively). This antioxidant effect could be involved in the anti-inflammatory effect described previously. Interestingly, the level of ROS in cells exposed to CeO<sub>2</sub> was lower as compared to those in cells exposed to TiO<sub>2</sub> and ZrO<sub>2</sub>, which is in accordance with antioxidant properties of CeO<sub>2</sub> described previously<sup>12</sup>. Since the pristine CeO<sub>2</sub> NPs possess antioxidant properties, the effect of Au deposited on CeO<sub>2</sub> was probably limited.

## Discussion

The most important result of this study is an anti-inflammatory effect of Au/MOx NPs depending on the MOx nature with particle internalization but no alteration of cell viability or phagocytic capacity of Au/MOx NPs as compared to MOx NPs (Figs. 2 and 3). The effect of Au/TiO<sub>2</sub> NPs was not related to Au NPs size (at least in the case of Au/TiO<sub>2</sub> NPs in the range of 3–8 nm) (Fig. 4) and was dependent on the MOx NPs chemical nature (Au/TiO<sub>2</sub> > Au/ZrO<sub>2</sub> > Au/CeO<sub>2</sub> if we consider the number of cytokines whose concentration was reduced by the NPs) and on the inflammatory mediator considered (Fig. 5). To the best of our knowledge, this is the first demonstration that Au/MOx presents anti-inflammatory properties.

The effect of Au/MOx could be related to anti-inflammatory properties of Au NPs per se. Indeed, gold colloids have been thought to cure various diseases for many centuries, and recent studies have demonstrated that this effect is mediated by inhibition of NF- $\kappa$ B activation<sup>13</sup>. Different studies showed a similar effect in the case of Au NPs in vitro and in vivo, this effect being usually mediated by antioxidant properties<sup>14–16</sup>. However, other studies showed opposite results. For example, Ng et al.<sup>16</sup> showed that incubation of human bronchial epithelial cells with 50  $\mu\text{g ml}^{-1}$  of 20 nm Au NPs activated NF- $\kappa$ B in bronchial epithelial cells. Close results were shown in other cell types<sup>17,18</sup>. Therefore, an anti-inflammatory effect of Au NPs per se seems not a univocal mechanism explaining the anti-inflammatory effect of Au/MOx NPs. Moreover, most of the studies showing the effect of Au NPs on inflammation have been conducted at much higher concentrations than the cells were exposed to in this study. Considering that Au NPs account for only 1% of the mass of Au/MOx, simply attributing the present results to the biological activity of Au NPs is unlikely.

Adsorption of TNF- $\alpha$  and IL-1 $\beta$  on Au/MOx surface could also explain their different anti-inflammatory activity. Indeed, NPs, including Au NPs, can adsorb different molecules on their surface, resulting in their inactivation and reduction in their concentration in the medium<sup>19</sup>. However, this mechanism seems unlikely in the present study, since we did not observe any significant difference in TNF- $\alpha$  and IL-1 $\beta$  levels when these cytokines were incubated with TiO<sub>2</sub> or ZrO<sub>2</sub> NPs and their respective Au counterparts (Fig. 6).

Finally, the differences in the anti-inflammatory effect of Au/MOx NPs could be related to their different antioxidant properties. However, the anti-inflammatory effect of Au/MOx NPs was not good consistent with the



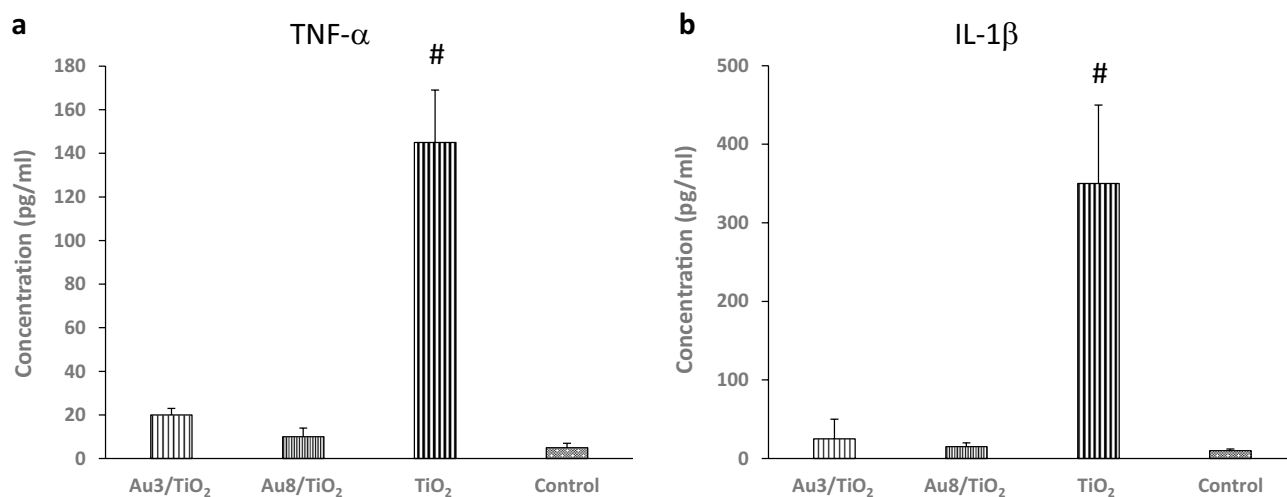


**Figure 4.** Effect of Au<sub>3</sub>/TiO<sub>2</sub>, Au<sub>8</sub>/TiO<sub>2</sub> and TiO<sub>2</sub> NPs (50 μg ml<sup>-1</sup>, 6 h incubation) on TNF-α and IL-1β secretion by mouse peritoneal macrophages (a,b). Data are expressed as picograms/ml in cell culture medium and are represented as mean ± SEM of 6 independent experiments. <sup>#</sup>Significantly different from control (*p* < 0.01).

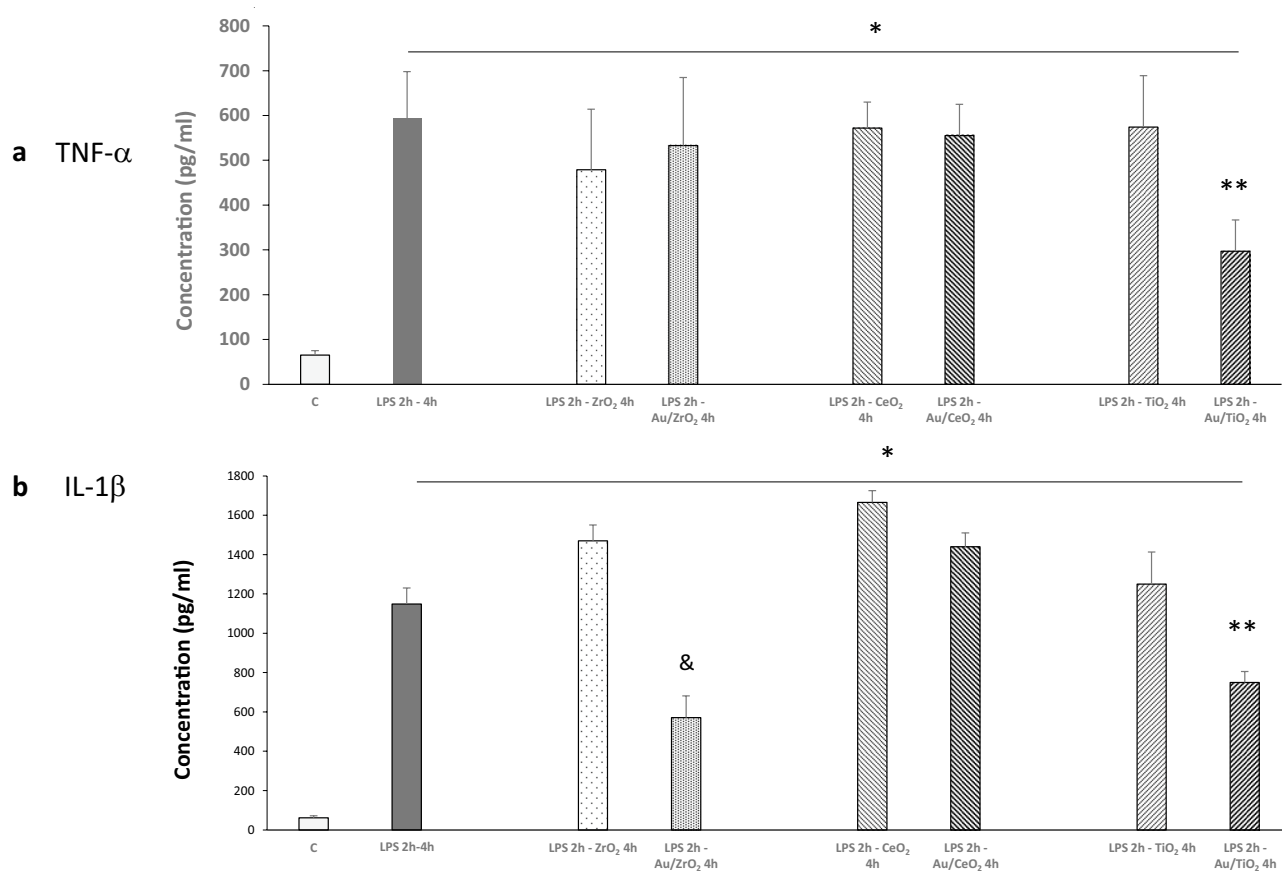


**Figure 5.** Effect of Au deposited on different metal oxide NPs on LPS induced TNF-α and IL-1β secretion by mouse peritoneal macrophages (a,b). Cells were incubated with culture media for 6 h (control condition, C) or LPS for 2 h, and then the following 4 h with LPS alone or LPS plus the different MOx or Au/MOx NPs (50 μg ml<sup>-1</sup>). <sup>\*</sup>Significantly different from C (*p* < 0.05), <sup>\*\*</sup>significantly different from LPS 2 h—TiO<sub>2</sub> 4 h (*p* < 0.05), <sup>&</sup>significantly different from LPS 2 h—ZrO<sub>2</sub> 4 h (*p* < 0.05).

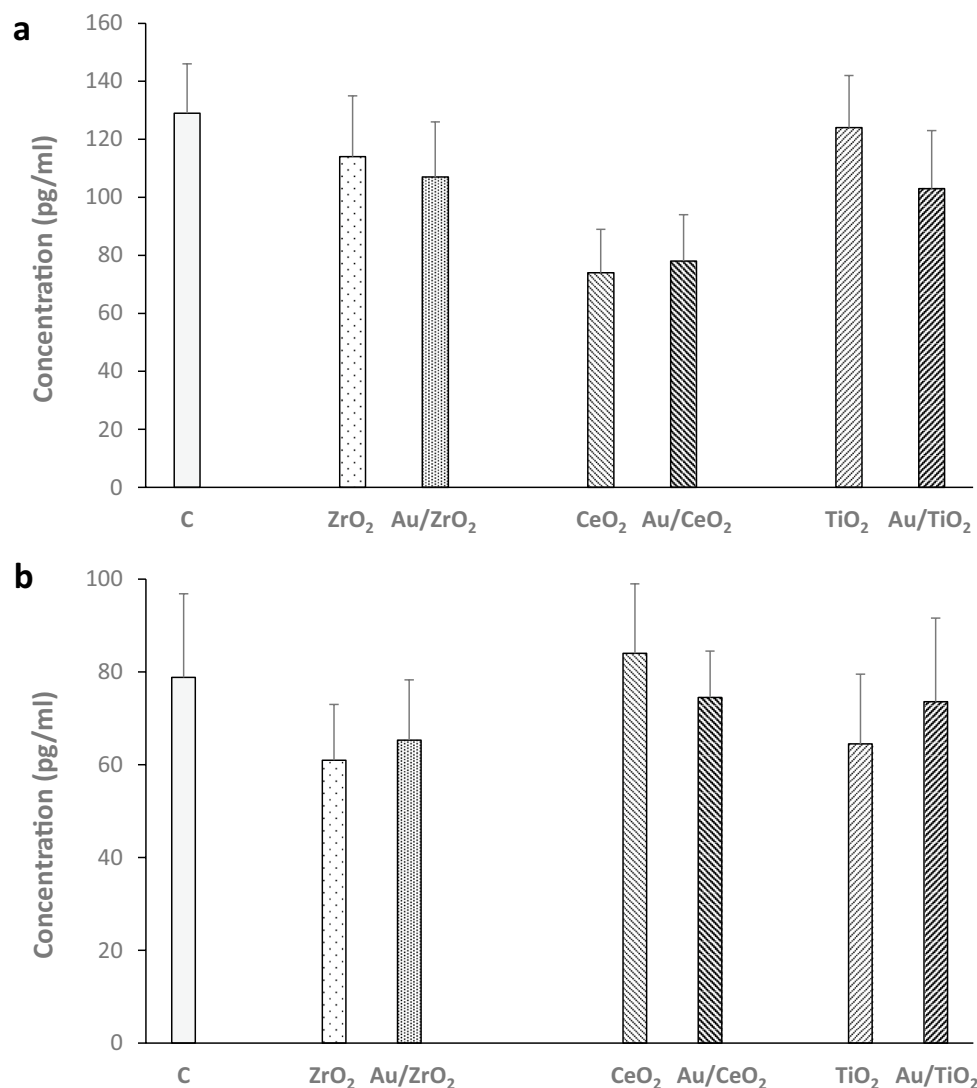


**Figure 6.** TNF- $\alpha$  and IL-1 $\beta$  adsorption on Au deposited on different MOx NPs. MOx or Au/MOx NPs ( $50 \mu\text{g ml}^{-1}$ ) were incubated during 6 h with TNF- $\alpha$  ( $150 \text{ pg ml}^{-1}$ ) and IL-1 $\beta$  ( $100 \text{ pg ml}^{-1}$ ) in culture media, then the cytokines were quantified in the media after centrifugation.

intracellular antioxidant properties, since both Au/TiO<sub>2</sub> and Au/ZrO<sub>2</sub> NPs reduced intracellular ROS concentration whereas only Au/TiO<sub>2</sub> attenuated both TNF- $\alpha$  and IL-1 $\beta$  induction (Fig. 5). In concordance with different studies, CeO<sub>2</sub> NPs exerted an antioxidant effect as compared to TiO<sub>2</sub> and ZrO<sub>2</sub> NPs (Table 1), but this effect was not accompanied by an anti-inflammatory effect. On the other hand, the absence of an anti-inflammatory effect of Au/CeO<sub>2</sub> was paralleled by an absence of an antioxidant effect of CeO<sub>2</sub> NPs. Collectively, these data suggest that, in contrast with our initial hypothesis, an antioxidant effect is not a mechanism globally explaining the anti-inflammatory effect of Au/TiO<sub>2</sub> and Au/ZrO<sub>2</sub>. Indeed, an antioxidant effect could potentially explain the effect of Au/TiO<sub>2</sub> NPs but not the one of Au/ZrO<sub>2</sub> NPs, because Au/ZrO<sub>2</sub> NPs had showed an antioxidant effect similar to Au/TiO<sub>2</sub> but attenuated only IL-1 $\beta$  induction. Consequently, the anti-oxidant effect of Au/ZrO<sub>2</sub> appears to relate to pathways inhibiting IL-1 $\beta$  but not TNF- $\alpha$  expression.

Numerous mechanisms have been reported to control the production and activity of IL-1 $\beta$ , including the processing of the 31-kDa, inactive IL-1 $\beta$  precursor into the bioactive, 17-kDa cytokine via intracellular protein complexes termed the inflammasomes<sup>20</sup>. The most intensely studied inflammasome is the NLRP3 inflammasome. Various stimuli activate the NLRP3 inflammasome: bacterial structures such as muramyl dipeptide or LPS, bacterial RNA,  $\beta$ -glucan, double-stranded RNA, etc. The release of ROS has been reported to mediate NLRP3 inflammasome activation by various stimuli, including LPS, but this has been surrounded by controversy<sup>21</sup>. Other proposed mechanisms responsible for NLRP3 inflammasome activation are: (i) translocation to mitochondria<sup>22</sup>, (ii) release of mitochondrial DNA or cardiolipin<sup>23</sup>, (iii) release of lysosomal cathepsins into the cytoplasm<sup>24</sup>, and (iv) calcium-dependent phospholipase 2 activation<sup>20</sup>. Interference with one or several mechanisms could explain attenuation of LPS-induced IL-1 $\beta$  expression by Au/ZrO<sub>2</sub> NPs. However, investigating these possibilities needs further studies.

This study presents four main limitations. First, as MOx NPs are made of different materials, the cells will be exposed to a different amount of particles. However, we consider this possibility unlikely because Au content in the different Au/MOx NPs was very low (around 1 wt%). Second, we used two different murine macrophages populations: primary cultures of peritoneal macrophages and the RAW 264.7 macrophages cell line. We chose to use primary cultures of peritoneal macrophages because a large body of literature combining both in vitro approaches using peritoneal macrophages, and in vivo experiments in mice, demonstrated the relevance of the findings obtained in peritoneal macrophages, and their potential translation to what may occur in vivo<sup>25–27</sup>. Moreover, we wanted to be at most in accordance with the 3R's guidelines, and for this reason we performed the experiments with the murine macrophage cell line RAW 264.7. Indeed, as demonstrated by Maurya and coworkers<sup>28</sup>, RAW264.7 cells behave similarly to primary cultures of peritoneal macrophages cells in some ways and can be used as a good model for inflammation- and immune function-related kinetic studies. RAW 264.7 behave different from peritoneal macrophages in other aspects of lipid metabolism and phenotypes used as models for various disorders such as atherosclerosis, but these types of responses were not concerned in the present study. Third, we only measured two cytokines as a surrogate of inflammatory markers. Even if these cytokines are broadly representative of the inflammatory reaction and are one of the very early ones in the inflammatory cascade, and we investigate primary murine macrophages (a key cell involved in inflammation), a wider analysis of mediators of this reaction is necessary to validate the present results. Fourth, we investigated only three MOx NPs supports. Although we choose supports widely characterized in terms of catalytic properties when combined with Au NPs, investigating a broader panel of MOx could allow a better characterizing the anti-inflammatory properties of Au/MOx NPs.

In conclusion, despite of the above-mentioned limitations, this study showed that Au/MOx possess anti-inflammatory properties in macrophages and the effect depended on the kind of MOx NPs. Au/TiO<sub>2</sub> showed anti-inflammatory effect for both TNF- $\alpha$  and IL-1 $\beta$ . Although Au/ZrO<sub>2</sub> was ineffective to reduce the concentration of TNF- $\alpha$ , the anti-inflammatory effect for IL-1 $\beta$  was more pronounced for Au/ZrO<sub>2</sub> as compared to Au/TiO<sub>2</sub>. In addition, Au/TiO<sub>2</sub> and Au/ZrO<sub>2</sub> exhibited improved antioxidant properties in RAW 264.7 compared to the pristine TiO<sub>2</sub> and ZrO<sub>2</sub> NPs. Although the relationships between antioxidant properties and anti-inflammatory effect of Au/MOx NPs and the mechanism are still unclear, our finding, anti-inflammatory effect of Au/MOx NPs could have potential applications in the clinical setting, since it does not interfere with physiological parameters of these cells such as viability and phagocytosis.

## Methods

**Preparation of Au nanoparticles supported on metal oxides (Au/MOx).** *Materials.* TiO<sub>2</sub> (AER-OXIDE P25) was supplied from Nippon Aerosil Co., Ltd. ZrO<sub>2</sub> (RC-100) and CeO<sub>2</sub> (high purity fine cerium oxide) were purchased from Daiichi Kigenso Kagaku Kogyo Co., Ltd. Tetrachloroauric acid (HAuCl<sub>4</sub>·4H<sub>2</sub>O) and dimethyl gold(III)(acetylacetonate), Me<sub>2</sub>Au(acac), were purchased from Tanaka Kikinzo Kogyo K.K. and Tri Chemical Laboratories Inc., respectively. Au/ZrO<sub>2</sub> and Au/CeO<sub>2</sub> prepared by deposition–precipitation were purchased from Haruta Gold Inc. All reagents and materials were used as received.

*Characterization of Au/MOx.* Average particle size of metal oxides after the deposition of Au NPs were measured by laser diffraction/scattering particle size distribution analyzer using a HORIBA, Partica LA-950V2. Specific surface area of metal oxides was estimated from the N<sub>2</sub> adsorption measurement was carried out using a SHIMADZU, Tristar 3000. The samples were pretreated at 200 °C for 2 h under vacuum, and then the N<sub>2</sub> adsorption isotherms were obtained at –196 °C. The Brunauer–Emmet–Teller (BET) method was used to calculate the specific surface area. Loading amount of Au on metal oxides were measured by inductively coupled plasma atomic emission spectroscopy (ICP-AES, Thermo Fisher Scientific, iCAP6500) or atomic absorption spectrometry (AAS, SHIMADZU, AA-6200). The samples were treated in aqua regia to dissolve Au NPs, filtered, and then diluted to measure. Average size of Au NPs supported on metal oxides were estimated by high-angle annular dark-field scanning transmission electron microscopic (HAADF-STEM) observation using a JEOL, JEM-3200FS.

*Preparation of Au/MOx.* Au NPs with two different mean diameters (3 and 8 nm) supported on pristine TiO<sub>2</sub> NPs were prepared, termed Au3/TiO<sub>2</sub> and Au8/TiO<sub>2</sub>, respectively. Au3/TiO<sub>2</sub> was prepared by deposition–precipitation<sup>3</sup>. An aqueous solution of HAuCl<sub>4</sub> (1 mM, 50 mL) was warmed to 70 °C, and the pH was adjusted to 6 by adding NaOH aqueous solution. TiO<sub>2</sub> (1.0 g) was added to the solution and the suspension was stirred at 70 °C for 1 h. The suspension was centrifuged, washed with water at 40 °C for five times, and then filtered. The resultant powder was dried in air at 100 °C overnight and calcined at 300 °C for 4 h to reduce Au(III) to Au(0). Au/ZrO<sub>2</sub> and Au/CeO<sub>2</sub> were also prepared by deposition–precipitation as well as Au3/TiO<sub>2</sub>. Au8/TiO<sub>2</sub> was prepared by solid grinding<sup>5</sup>. TiO<sub>2</sub> (1.0 g) and Me<sub>2</sub>Au(acac) (15 mg) were ground in an agate mortar in air at room temperature for 20 min. The mixture was calcined at 300 °C for 2 h to give Au8/TiO<sub>2</sub>.

Physicochemical properties of the obtained Au/MOx are summarized in Table 1. The primary particle sizes of Au/TiO<sub>2</sub>, Au/ZrO<sub>2</sub>, and Au/CeO<sub>2</sub> were 26 nm, 11 nm, and 7.3 nm respectively, estimated from their specific surface areas of the MOx NPs. The secondary particle sizes of Au/TiO<sub>2</sub>, Au/ZrO<sub>2</sub>, and Au/CeO<sub>2</sub> were 9.4  $\mu$ m, 3.6  $\mu$ m, and 2.4  $\mu$ m, respectively, determined by light scattering. The actual Au loadings for Au3/TiO<sub>2</sub>, Au8/TiO<sub>2</sub>, Au/ZrO<sub>2</sub>, and Au/CeO<sub>2</sub> were 0.96, 1.18, 0.97, and 0.96 wt%, respectively. The mean diameters of Au NPs were estimated by HAADF-STEM observation to be 3.3  $\pm$  1.4 nm for Au3/TiO<sub>2</sub>, 7.8  $\pm$  2.7 nm for Au8/TiO<sub>2</sub>, and 3.3  $\pm$  1.8 nm for Au/ZrO<sub>2</sub> (Fig. 1). In the case of Au/CeO<sub>2</sub>, it was difficult to observe Au NPs because Au was mostly deposited as single atoms and the atomic number of Ce is close to that of Au.



The different NPs were evaluated for LPS contamination (Limulus Amebocyte Lysate test), and the observed absorbance at 405 nm was below detection limits demonstrating no LPS contamination.

**Cells isolation and incubation with nanoparticles.** Peritoneal macrophages and macrophages from the RAW 264.7 cell line were used in the different experiments.

Mice peritoneal macrophages were prepared as follows. C57BL/6 mice were injected intraperitoneally with 1 ml of 3% Brewer thioglycollate (Sigma-Aldrich, B2551). After 96 h, peritoneal cells were harvested by lavage with 0.67% phosphate buffered saline (PBS). After a soft centrifugation, cells were maintained in Dulbecco's modified Eagle medium (DMEM) 4.5 g l<sup>-1</sup> glucose supplemented with 10% fetal calf serum (FCS) and 1% penicillin and 1% streptomycin. Then mice peritoneal macrophagic cells were exposed for 6–48 h to 1–100 µg ml<sup>-1</sup> particles of Au/TiO<sub>2</sub>, Au/ZrO<sub>2</sub>, Au/CeO<sub>2</sub>, and MOx alone.

The RAW 264.7 cells were cultured using a medium having the same composition as above.

Nanoparticle interference with the signal was tested in all of the colorimetric assays. No interference was observed.

**Cellular viability.** The viability of cells was measured by 3-[4,5-dimethylthiazol-2-yl]-2,5 diphenyl tetrazolium bromide (MTT) assay, 2-(4-iodophenyl)-3-(4-nitrophenyl)-5-(2,4-disulphophenyl)-2H-tetrazolium, monosodium salt (WST-1) assay, and the quantification of the release of lactate dehydrogenase (LDH).

**Inflammatory responses.** Inflammatory response was evaluated by the quantification of cytokines such as tumor necrosis factor (TNF)-α and interleukin (IL)-1β in cell supernatant, measured by enzyme-linked immunosorbent assay (ELISA).

**Measurement of oxidative stress by DCFH-DA assay.** Endogenous ROS were quantified by oxidation of 2',7'-dichlorofluorescein diacetate (DCFH-DA) into 2',7'-dichlorofluorescein (Sigma, Saint Quentin Fallavier, France). Briefly, cells were cultivated in six-well culture plates and treated with 50 µg ml<sup>-1</sup> NPs. Cells were also treated with 250 µM H<sub>2</sub>O<sub>2</sub> as a positive control (data not shown). Cells were incubated with 20 µM DCFH-DA for 30 min at 37 °C and fluorescence recorded for 90 min. Results were expressed as the mean ratio of fluorescence recorded every 15 min during the 90 min period.

**Measurement of TNF-α and IL-1β adsorption to NPs.** Adsorption of TNF-α and IL-1β adsorption to NPs was performed by ELISA as described previously described<sup>29</sup>.

**Statistical analysis.** JASP software (version 0.11.1, <https://jasp-stats.org/>) was used to analyze quantitative data. Non-parametric ANOVA was used to compare multiple groups. Paired comparisons with Mann–Whitney test were performed if the differences using ANOVA were statistically significantly different. Data were presented as mean values ± standard error of the mean (SEM), and results were considered statistically significant if  $p < 0.05$ .

**Study approval for animal experiments.** The Institutional Animal Care and Use Committee approved experimental procedures on mice (APAFIS authorization #14914-2018042515599016).

All methods were carried out in accordance with relevant guidelines and regulations and are reported in accordance with ARRIVE guidelines for the reporting of animal experiments.

## Data availability

The datasets used and/or analyzed during the current study are available from the corresponding author on reasonable request.

Received: 12 February 2021; Accepted: 2 November 2021

Published online: 30 November 2021

## References

- Haruta, M. When gold is not noble: Catalysis by nanoparticles. *Chem. Rec.* **3**(2), 75–87 (2003).
- Taketoshi, A. & Haruta, M. Size- and structure-specificity in catalysis by gold clusters. *Chem. Lett.* **43**, 380–387. <https://doi.org/10.1246/cl.131232> (2014).
- Haruta, M. *et al.* Low-temperature oxidation of Co over gold supported on TiO<sub>2</sub>, AlphaFe<sub>2</sub>O<sub>3</sub>, and Co<sub>3</sub>O<sub>4</sub>. *J. Catal.* **144**, 175–192. <https://doi.org/10.1006/jcat.1993.1322> (1993).
- Ishida, T., Murayama, T., Taketoshi, A. & Haruta, M. Importance of size and contact structure of gold nanoparticles for the genesis of unique catalytic processes. *Chem. Rev.* **120**(2), 464–525 (2020).
- Ishida, T. *et al.* Influence of the support and the size of gold clusters on catalytic activity for glucose oxidation. *Angew. Chem. Int. Ed.* **47**(48), 9265–9268 (2008).
- Ishida, T. & Haruta, M. Gold catalysts: Towards sustainable chemistry. *Angew. Chem. Int. Ed.* **46**(38), 7154–7156 (2007).
- Menchón, C. *et al.* Gold nanoparticles supported on nanoparticulate ceria as a powerful agent against intracellular oxidative stress. *Small Weinh Bergstr Ger.* **8**(12), 1895–1903 (2012).
- Tuder, R. M., Davis, L. A. & Graham, B. B. Targeting energetic metabolism: A new frontier in the pathogenesis and treatment of pulmonary hypertension. *Am. J. Respir. Crit. Care Med.* **185**(3), 260–266 (2012).
- Lundqvist, M. *et al.* Nanoparticle size and surface properties determine the protein corona with possible implications for biological impacts. *Proc. Natl. Acad. Sci. U S A.* **105**(38), 14265–14270 (2008).
- Lucchetti, B. F. C. *et al.* Metabolic syndrome aggravates cardiovascular, oxidative and inflammatory dysfunction during the acute phase of *Trypanosoma cruzi* infection in mice. *Sci. Rep.* **9**(1), 18885 (2019).

11. Scalavino, V. *et al.* miR-369-3p modulates inducible nitric oxide synthase and is involved in regulation of chronic inflammatory response. *Sci. Rep.* **10**(1), 15942 (2020).
12. Pezzini, I. *et al.* Cerium oxide nanoparticles: The regenerative redox machine in bioenergetic imbalance. *Nanomedicine* **12**(4), 403–416 (2017).
13. Narayanan, K. B. & Park, H. H. Pleiotropic functions of antioxidant nanoparticles for longevity and medicine. *Adv. Colloid Interface Sci.* **201–202**, 30–42 (2013).
14. Zhu, S. *et al.* Orally administered gold nanoparticles protect against colitis by attenuating Toll-like receptor 4- and reactive oxygen/nitrogen species-mediated inflammatory responses but could induce gut dysbiosis in mice. *J. Nanobiotechnol.* **16**(1), 86 (2018).
15. Pereira, D. V. *et al.* Effects of gold nanoparticles on endotoxin-induced uveitis in rats. *Invest. Ophthalmol. Vis. Sci.* **53**(13), 8036–8041 (2012).
16. Hauptenthal, D. P. D. S. *et al.* Effects of chronic treatment with gold nanoparticles on inflammatory responses and oxidative stress in Mdx mice. *J. Drug Target.* **28**(1), 46–54 (2020).
17. Khan, H. A., Abdelhalim, M. K., Alhomida, A. S. & Al Aayed, M. S. Transient increase in IL-1 $\beta$ , IL-6 and TNF- $\alpha$  gene expression in rat liver exposed to gold nanoparticles. *Genet. Mol. Res. GMR* **12**(4), 5851–5857 (2013).
18. Li, Y. *et al.* Bacterial endotoxin (lipopolysaccharide) binds to the surface of gold nanoparticles, interferes with biocorona formation and induces human monocyte inflammatory activation. *Nanotoxicology* **11**(9–10), 1157–1175 (2017).
19. Mukherjee, P. *et al.* Antiangiogenic properties of gold nanoparticles. *Clin. Cancer Res.* **11**(9), 3530–3534 (2005).
20. Lamkanfi, M. & Dixit, V. M. Mechanisms and functions of inflammasomes. *Cell* **157**(5), 1013–1022 (2014).
21. Netea, M. G., van de Veerdonk, F. L., van der Meer, J. W. M., Dinarello, C. A. & Joosten, L. A. B. Inflammasome-independent regulation of IL-1-family cytokines. *Annu. Rev. Immunol.* **33**, 49–77 (2015).
22. Subramanian, N., Natarajan, K., Clatworthy, M. R., Wang, Z. & Germain, R. N. The adaptor MAVS promotes NLRP3 mitochondrial localization and inflammasome activation. *Cell* **153**(2), 348–361 (2013).
23. Nakahira, K. *et al.* Autophagy proteins regulate innate immune responses by inhibiting the release of mitochondrial DNA mediated by the NALP3 inflammasome. *Nat. Immunol.* **12**(3), 222–230 (2011).
24. Duewell, P. *et al.* NLRP3 inflammasomes are required for atherogenesis and activated by cholesterol crystals. *Nature* **464**(7293), 1357–1361 (2010).
25. Tabet, L. *et al.* Coating carbon nanotubes with a polystyrene-based polymer protects against pulmonary toxicity. *Part Fibre Toxicol.* **21**(8), 3 (2011).
26. Hevia, H. *et al.* 5'-methylthioadenosine modulates the inflammatory response to endotoxin in mice and in rat hepatocytes. *Hepatology* **39**(4), 1088–1098 (2004).
27. Bachoual, R. *et al.* Biological effects of particles from the paris subway system. *Chem. Res. Toxicol.* **20**(10), 1426–1433 (2007).
28. Maurya, M. R. *et al.* Analysis of inflammatory and lipid metabolic networks across RAW264.7 and thioglycolate-elicited macrophages. *J. Lipid Res.* **54**(9), 2525–2542 (2013).
29. Bussy, C. *et al.* Critical role of surface chemical modifications induced by length shortening on multi-walled carbon nanotubes-induced toxicity. *Part Fibre Toxicol.* **9**, 46 (2012).

## Acknowledgements

This work is financially supported by JSPS KAKENHI Grant Number JP19K15410.

## Author contributions

T.F. prepared and analyzed NPs, performed chemical experiments and critically reviewed the manuscript. T.F., M.Z. and D.E. performed biological experiments. T.M., M.H., and S.L. critically reviewed the manuscript and worked on its final elaboration. T.I. contributed to the design of the study, critically reviewed the manuscript and worked on its final elaboration. J.B. designed the study and wrote the first and final drafts of the manuscript. All authors approved the final version of the manuscript.

## Competing interests

The authors declare no competing interests.

## Additional information

**Supplementary Information** The online version contains supplementary material available at <https://doi.org/10.1038/s41598-021-02419-4>.

**Correspondence** and requests for materials should be addressed to T.F. or J.B.

**Reprints and permissions information** is available at [www.nature.com/reprints](http://www.nature.com/reprints).

**Publisher's note** Springer Nature remains neutral with regard to jurisdictional claims in published maps and institutional affiliations.



**Open Access** This article is licensed under a Creative Commons Attribution 4.0 International License, which permits use, sharing, adaptation, distribution and reproduction in any medium or format, as long as you give appropriate credit to the original author(s) and the source, provide a link to the Creative Commons licence, and indicate if changes were made. The images or other third party material in this article are included in the article's Creative Commons licence, unless indicated otherwise in a credit line to the material. If material is not included in the article's Creative Commons licence and your intended use is not permitted by statutory regulation or exceeds the permitted use, you will need to obtain permission directly from the copyright holder. To view a copy of this licence, visit <http://creativecommons.org/licenses/by/4.0/>.

© The Author(s) 2021